Biochemical and Biophysical Research Communications 441 (2013) 351–356

Contents lists available at ScienceDirect

Biochemical and Biophysical Research Communications

journal homepage: www.elsevier.com/locate/ybbrc

Blockade of SOCE protects HT22 cells from hydrogen peroxide-induced apoptosis

Wei Rao [1], Lei Zhang [1], Ning Su [1], Kai Wang, Hao Hui, Li Wang, Tao Chen, Peng Luo, Yue-fan Yang, Zao-bin Liu, Zhou Fei *

Department of Neurosurgery, Xijing Hospital, Fourth Military Medical University, Xi'an 710032, PR China

ARTICLE INFO

Article history:
Received 9 October 2013
Available online 22 October 2013

Keywords:
Reactive oxygen species
Mitochondria
Apoptosis
Calcium homeostasis
SOCE

ABSTRACT

Oxidative stress is an established event in the pathology of neurobiological diseases. Previous studies indicated that store-operated Ca^{2+} entry (SOCE) has been involved in oxidative stress. The present study was carried out to investigate the effects of SOCE inhibition on neuronal oxidative stress injury induced by hydrogen peroxide (H_2O_2) in HT22 cells, a murine hippocampal neuronal model. H_2O_2 insult induced significant intracellular Ca^{2+} overload, mitochondrial dysfunction and cell viability decrease. Inhibition of SOCE by pharmacological inhibitor and STIM1 RNAi significantly alleviated intracellular Ca^{2+} overload, restored the mitochondrial membrane potential (MMP), decreased cytochrome C release and eventually inhibited H_2O_2-induced cell apoptosis. These findings suggest that SOCE inhibition exhibited neuroprotection against oxidative stress induced by H_2O_2 and SOCE might be a useful therapeutic target in neurobiological disorders.

1. Introduction

The production and elimination of ROS, such as superoxide anion (O^{2-}) and hydrogen peroxide (H_2O_2), play an important role in normal physiological function but need sophisticated regulation. Loss of the homeostasis between production and clearance of ROS could induce oxidative stress and lead to cell death through apoptotic, necrotic, and necroptotic pathways. Growing evidence indicated that oxidative stress was involved in several neurodegenerative disorders [1,2], as well as in stroke [3], trauma [4], and seizures [5,6]. Therefore, abundant researches focused on the mechanisms and role of oxidative stress in neurobiological diseases.

Ca^{2+}, as a ubiquitous second messenger, is involved in a plethora of cellular functions including energy metabolism and cell death and has tight relationships with oxidative signaling [7]. SOCE, which was mediated by the sensor stromal interactive molecules (STIM) and Ca^{2+} release-activated Ca^{2+} channel (CACc), has a tight relationship with Ca^{2+} homeostasis by sensing endoplasmic reticulum (ER) Ca^{2+} level and mediating extracellular Ca^{2+} entry to raise cytosolic Ca^{2+} and to refill Ca^{2+} store [8]. Recently, some researches indicated that SOCE was extensively involved in oxidative stress of non-excited cells, such as endothelial cells [9], embryonic fibroblast cells [7], T cells [10]. However, under different pathophysiological settings, whether SOCE had a protective or detrimental role is still on inconsistent. Some reports showed that SOCE contributed to Ca^{2+} overload and followed cell death, including STIM1 signaling- [9] and Orai1-mediated Ca^{2+} entry [11]. In contrast, several studies indicated that intact SOCE machinery was necessary to cell survival through balancing energy production, detoxificating ROS [7], regulating Ca^{2+} homeostasis and inhibiting the unfolded protein response (UPR) [12]. Furthermore, the role of SOCE in oxidative stress injury of excited cells, especially in neurons, was poorly investigated.

In this study, we applied HT22 cells to investigate the effect of SOCE on neuronal oxidative stress induced by H_2O_2 application. We found that inhibition of SOCE by pharmacological inhibition and genetically interfere STIM1 expression alleviated cell calcium overload, mitochondrial dysfunction and apoptotic cell death, suggesting that SOCE inhibition might be a valuable tool in the treatment of oxidative stress associated neurological diseases.

2. Materials and methods

2.1. Cell culture

The HT22 cell line was obtained from the Institute of Biochemistry and Cell Biology, SIBS, CAS. The cell line was cultured in DMEM high glucose (Gibco), supplemented with 10% fetal bovine serum (PAA Laboratories) in a humidified incubator with 5% CO_2 and 95% air. One day before experiments, cells were seeded in 6-well culture dishes at $1*10^6$ per well.

* Corresponding author. Fax: +86 29 84775567.
E-mail address: feizhou@fmmu.edu.cn (Z. Fei).
[1] These authors contributed equally to this work.

0006-291X/$ - see front matter © 2013 Elsevier Inc. All rights reserved.
http://dx.doi.org/10.1016/j.bbrc.2013.10.054

2.2. Cell viability assay

Cell viability assay was performed by using cell counting kit-8 (CCK-8) (Dojindo) following the manufacture's protocol. HT22 cells were seeded in a 96-well with 100 μl/well culture medium (5000 cells/well) and cultured in a humidified incubator for 24 h. Lentivirus shRNA-infected cells were seeded 72 h post infection. 2-APB (Sigma) were added before H_2O_2 (Sigma) application. Cell viability was quantified 12 h after stress onset with 10 μl/well of WST-8 solution. After 4 h incubation in the incubator, the absorbance at 450 nm was measured using a microplate reader (Bio-Rad). Cell viability was expressed as a percentage of the control group.

2.3. Measurement of cytosolic Ca^{2+} concentration ($[Ca^{2+}]_{cyt}$) and MMP

HT22 cells were seeded in 20 mm Confocal Petri Dish (Nest) and loaded with Fluo-4 AM (3 μM) or TMRM (50 nM) (Molecular Probe) in Hanks Balanced Salt Solution supplemented with 20 mM D-glucose and 10 mM HEPES (HBSS) (Gibco) for 45 min, and equilibrated for 30 min in dark. Then, cells were mounted on the stage of a confocal laser scanning microscope (FV10i, Olympus), and the fluorescence changes were determined in an XYT-plane fashion. Fluo-4 AM was excited at 488 nm and the emission was collected through a 505–550 nm barrier filter; TMRM was excited at 543 nm, and the emission was collected through a 560 nm long-pass filter. Signals from different groups were compared using identical settings for laser power and detector sensitivity for each separate experiment. After 10 min of baseline recording or additional 20 min of inhibitor incubation, 750 μM H_2O_2 was added in the solution. The images were acquired with Olympus confocal software and analyzed using Image J (National Institutes of Health).

2.4. Real-time RT-PCR

Total RNA was isolated after 72 h Lenti virus sh-RNA infection using Trizol (Invitrogen). A 2–3 mg template RNA was used to synthesize the first strand of cDNA using a reverse transcription kit (Takara). Real-time PCR of cDNA was performed using the forward and reverse primer sequences: STIM1: forward, 5′-TGA GGC CGT CCG AAA CAT C-3′; reverse, 5′-TCA CTG TTG GGT CAT GGT AAT TGA G-3′; GAPDH: forward, 5′-GGG TCA GAA GGA TTC CTA TG-3′; reverse, 5′-GGT CTC AAA CAT GAT CTG GG-3′. Data were analyzed using a comparative critical threshold (Ct) method where the amount of target normalized to the amount of endogenous control and relative to the control samples.

2.5. Plasmids and Lenti virus generation

Optimal STIM1 shRNA (5′-GCA GTA CTA CAA CAT CAA GAA-3′) or scramble shRNA (5′-UUC UCC GAA CGU GUC ACG U-3′) was cloned into the lentivirus-based RNAi vector pGCL vector and its sequence was confirmed by PCR and sequencing analysis. Lenti virus preparations were produced by the Shanghai GeneChem Co. Ltd, China. HT22 cells were infected by addition of Lenti virus into the cell culture at an MOI of approximately 40. Following 72 h infection, HT22 cells were subjected to various measurements.

2.6. Western blot

Western blot was analyzed as previously described [13]. The proteins extracted from HT22 cells were used for Western blot. The membranes were blocked and then incubated at 4 °C overnight with the appropriate primary antibody (STIM1, 1:2000; caspase-3, 1:1500; cleaved-caspase-3, 1:1000; Bcl-2, 1:800; Bax, 1:800; β-actin, 1:2000. Cell Signaling Technology). Immunoreactivity was detected by Chemiluminescent Substrate (Thermo Scientific). The optical densities of the bands were quantified by using Image J.

2.7. Flow cytometry

HT22 cells were harvested at 12 h after exposure to H_2O_2, washed, and then re-suspended in binding buffer. Cell suspension was transferred into a tube and double-stained for 15 min with Alexa Fluor 488-conjugated Annexin V (AV) and propidium iodide (PI) dye (Roche Applied Science) at RT in the dark. After addition of 400 ml binding buffer, the stained cells were analyzed by an FC500 flow cytometer with the fluorescence emission at 530 and 575 nm. The CXP cell quest software (Beckman–Coulter, USA) was used to count the number of cells and analyzed the results.

2.8. Quantification of cytochrome C release

Cytochrome C release into the cytoplasm was assessed as previously described [13]. The cytosolic fraction and mitochondrial fraction of HT22 cells were prepared though centrifuge. Then, the levels of cytochrome C in cytosolic and mitochondrial fractions were measured using the Quantikine M Rat/Mouse Cytochrome C Immunoassay kit obtained (R&D). Data were expressed as ng/mg protein.

2.9. Statistical analysis

The data are presented as $\bar{\chi} \pm$ SEM and statistical analysis was performed using SPSS 21.0. Statistical evaluation of the data was performed by one-way analysis of variance (ANOVA) followed by Bonferroni's multiple comparisons or unpaired t test (two groups). A value of $p < 0.05$ was considered statistically significant.

3. Results

3.1. H_2O_2 induced cytotoxicity and cell death in HT22 cells

HT22 cells were treated with H_2O_2 in different concentrations (100, 250, 500, 750, 1000, or 1250 μM) for 12 h. The cytotoxicity was assessed by using WST-8 and LDH release detection. We found that H_2O_2 insult significantly decreased cell viability and increased LDH release in a dose-dependent manner (Fig. 1A and B). Because 750 μM H_2O_2 induced approximate 50% cell viability decrease, it was used in the following experiments. Further, flow cytometry detection showed that 750 μM H_2O_2 insult significantly increased apoptotic cell death as compared with control group (Fig. 1C and D).

3.2. H_2O_2 insult induced cytotoxicity is partly dependent on $[Ca^{2+}]_{cyt}$ overload

Fluo-4 AM was used to monitor $[Ca^{2+}]_{cyt}$ changes after H_2O_2 insult. Fig. 1E shows dynamic changes of $[Ca^{2+}]_{cyt}$, expressed as a percentage of the baseline(F/F_0) for up to 2 h following H_2O_2 injury. H_2O_2 insult triggered a rapid rise in $[Ca^{2+}]_{cyt}$ within 45 min, which began to slowly decrease at 90 min, while there are no changes in control group. Then, BAPTA-AM (10 μM), an intracellular free-calcium chelator, was applied before H_2O_2 insult. As shown in Fig. 1F, BAPTA-AM application significantly alleviated cell death induced by H_2O_2, suggesting that H_2O_2 induced cytotoxicity and cell death was partially dependent on $[Ca^{2+}]_{cyt}$ overload.

3.3. Inhibition of SCOE limited H_2O_2-induced cytotoxicity and cell death

As verified by RT-PCR and Western blot, STIM1 expression levels were successfully downregulated compared to Control group

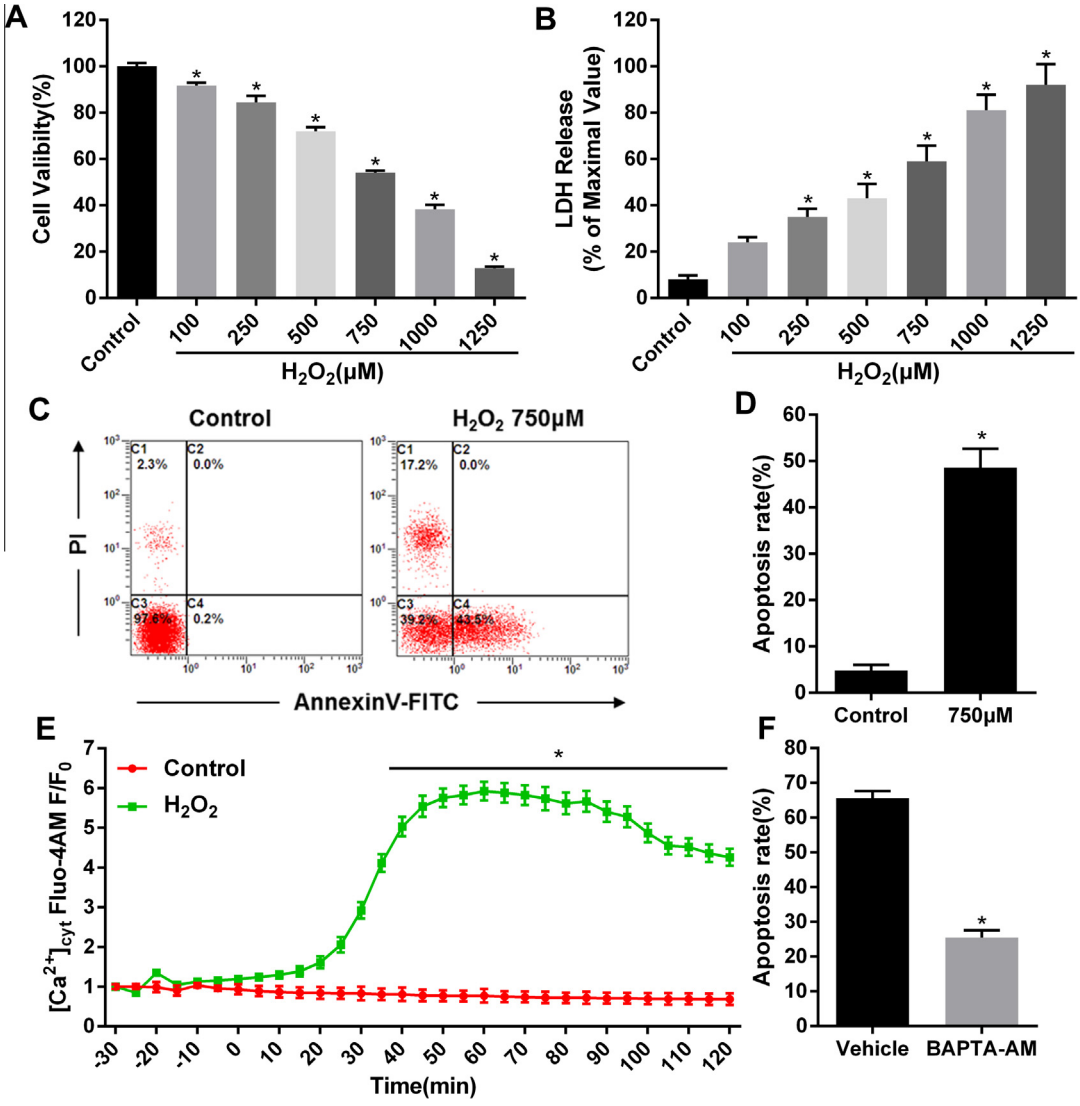

Fig. 1. H_2O_2-induced cell injury is partially dependent on Ca^{2+} overload in HT22 cells. HT22 cells were treated with H_2O_2 of different concentrations for 12 h, cell viability was measured by CCK-8 assay (A), and cytotoxicity was measured by LDH assay (B). HT22 cells were treated with 750 μM H_2O_2 for 12 h, and the percentage of apoptotic cells was analyzed using flow cytometry (AV^+/PI^+, the late phase apoptotic cells; AV^+/PI^-, the early phase apoptotic cells) (C and D). HT22 cells were treated with 750 μM H_2O_2 and the intracellular Ca^{2+} concentration $[Ca^{2+}]_{cyt}$ was measured by Fluo-4 AM Ca^{2+} indicator up to 120 min after injury (E). HT22 cells were pre-treated with BAPTA-AM (10 μM) or DMSO for 0.5 h before H_2O_2 (750 μM) insult, and cell death was measured by flow cytometry detection (F). The data were represented as mean ± SEM from five experiments. $^*p < 0.05$ vs Control or Vehicle group.

(Fig. 2A and B). HT22 cells were infected with LV-S1i/LV-Scr for 72 h or pretreated with 2-APB (75 μM, DMSO 0.5‰) 20 min before H_2O_2 addition. After H_2O_2 application for 12 h, CCK-8 assays results showed that 2-APB application significantly inhibited the decrease of cell viability induced by H_2O_2 insult compared Vehicle group (Fig. 2C). Similarly, compared with LV-Scr group, STIM1 RNAi also significantly alleviated the decrease of cell viability (Fig. 2C). Further, we clarified the CCK-8 result by flow cytometry Annexin V/PI staining detection (Fig. 2D), and the results showed that H_2O_2 induced apoptotic cell death was partly prevented by 2-APB or STIM1 RNAi.

3.4. Inhibition of SCOE alleviated H_2O_2-induced intracellular calcium overload

As SOCE had a tight relationship with intracellular Ca^{2+} dynamic equilibrium, we monitored $[Ca^{2+}]_{cyt}$ changes using Fluo-4 AM. Pretreatment with 2-APB significantly lower $[Ca^{2+}]_{cyt}$ overload level as compared to Vehicle group(Fig. 3A). Meantime, compared with LV-Scr group, STIM1 RNAi also significantly alleviated intracellular Ca^{2+} overload (Fig. 3B). Thus, limitation of SOCE by pharmacological inhibition and gene interfere approaches alleviated Ca^{2+} overload and delayed Ca^{2+} peak time.

3.5. Inhibition of SCOE protected H_2O_2-induced mitochondrial dysfunction and apoptosis

Mitochondrial dysfunction was intensively involved in oxidative stress. We found that inhibition of SOCE by 2-APB application exhibited a smaller percentage change in TMRM signal following H_2O_2 treatment compared with Vehicle group, indicating a greater reserve of MMP (Fig. 4A), and a similar pattern of MPP preservation in LV-S1i group was also observed (Fig. 4A). Meantime, compared with Vehicle or LV-Scr group, the release of cytochrome C into cytoplasm was also significantly decreased in 2-APB and LV-S1i group (Fig. 4B and C). Then, we detected the rate of Bax/Bcl-2 and Caspase 3 activation in H_2O_2 insulted HT-22 cells. As shown in Fig. 4, both 2-APB and LV-S1i application inhibited the increase of rate of Bax/Bcl-2 (Fig. 4D and E) and limited the activation of

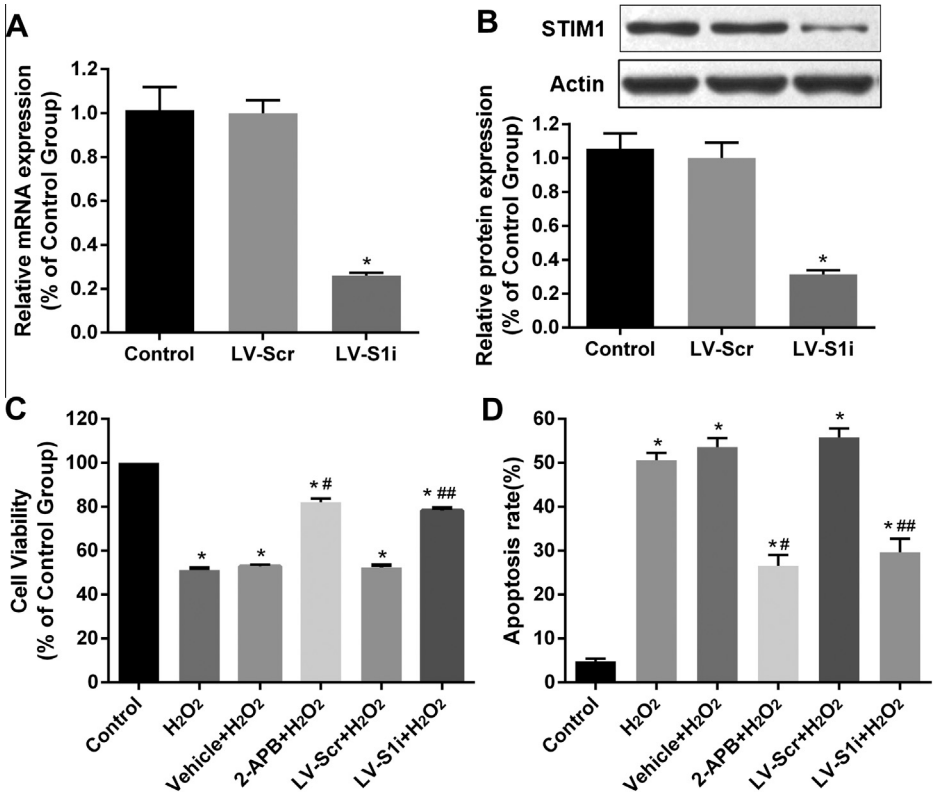

Fig. 2. Protect effect of SOCE inhibition on H_2O_2-induced cell injury. HT22 cells were infected with LV-S1i or LV-Scr for 72 h before H_2O_2 insult, and the expression of STIM1 was examined by qRT-PCR (A), and Western blot analysis (B). After pretreated with 2-APB (75 μM) for 20 min or successfully STIM1 RNAi, HT22 cells was treated with H_2O_2 for 12 h and cell viability was measured by CCK-8 assay (C), and cell apoptosis was measured by flow cytometry detection (D). The data were represented as mean ± SEM from five experiments. $^{*}p < 0.05$ vs Control group, $^{\#}p < 0.05$ vs Vehicle group, $^{\#\#}p < 0.05$ vs LV-Scr group.

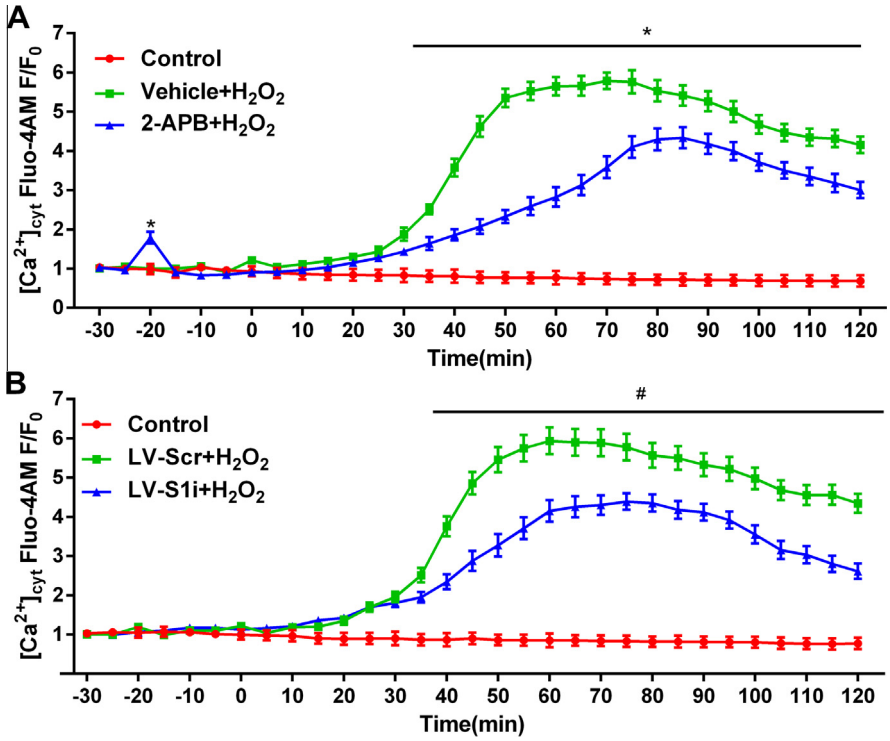

Fig. 3. Effect of SOCE inhibition on H_2O_2-induced cellular Ca^{2+} overload. HT22 cells were pre-treated with 75 μM 2-APB (−20 min) before H_2O_2 insult (0 min) and the intracellular Ca^{2+} concentration $[Ca^{2+}]_{cyt}$ was measured by Fluo-4 AM Ca^{2+} indicator up to 120 min (A). After infection of LV-S1i or LV-Scr for 72 h, HT22 cells were treated with H_2O_2, and $[Ca^{2+}]_{cyt}$ was measured by Fluo-4 AM Ca^{2+} indicator up to 120 min (B). The data were represented as mean ± SEM from four experiments. $^{*}p < 0.05$ vs Vehicle group, $^{\#}p < 0.05$ vs LV-Scr group.

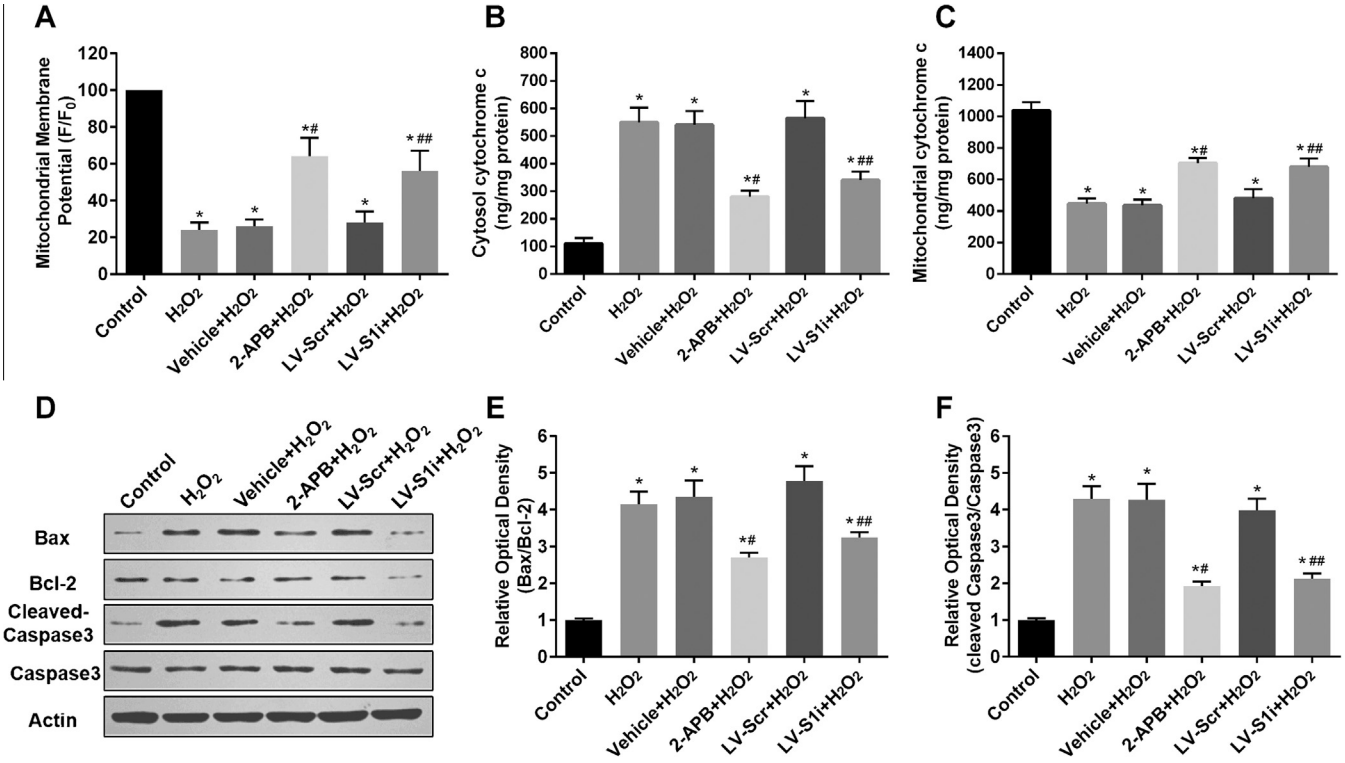

Fig. 4. Effect of SOCE inhibition on H_2O_2-induced MMP loss and mitochondrial-associated apoptosis. After pretreated with 2-APB (75 μM) for 20 min or successfully STIM1 RNAi, HT22 cells were treated with 750 μM H_2O_2. MMP was determined by TMRM (A), and the release of cytochrome C into the cytoplasm was determined by an immunoassay kit after subcellular fraction preparation (B and C). The expression of Bax, Bcl-2, cleaved-Caspase-3, and Caspase-3 were determined by Western blot analysis (D), and the ratio of Bax/Bcl-2 (E) and activity of Caspase-3 (F) were calculated. The data were represented as mean ± SEM from five experiments. $^{*}p < 0.05$ vs Control group, $^{\#}p < 0.05$ vs Vehicle group, $^{\#\#}p < 0.05$ vs LV-Scr group.

Caspase 3 (Fig. 4D and F). These results indicated that inhibition of SOCE attenuated H_2O_2-induced mitochondrial dysfunction and mitochondrial apoptosis.

4. Discussion

H_2O_2, a classic reactive oxygen species, is an source of hydroxyl free radicals normally produced in cells, including neurons [14]. It was extensively applied as an inducer of oxidative stress in in vitro model [15]. H_2O_2-challenged cells show typical morphological and biochemical characteristics of oxidative stress, including cellular swelling, vacuole degeneration, lipids and proteins oxidization, disturb of calcium hemostasis, and subsequently leading to cell death. Our study also used H_2O_2 to generate an in vitro model of oxidative stress and confirmed that H_2O_2 insult caused dose-dependently cell viability decrease. At the concentration of 750 μM, HT22 cells exhibited significant cell viability decrease, intracellular Ca^{2+} overload and apoptotic cell death. These results were in line with other researches including neurons [16–18].

SOCE has been extensively recognized as a primary mechanism to modulating Ca^{2+} homeostasis. Meantime, growing evidence indicated that SOCE extensively involved in oxidative stress [7,9,10]. Previous study showed that SOCE could be activated by calcium store-independent/ROS-dependent or store-dependent STIM1 activation when ROS was elevated [11,19,20]. However, the role of SOCE in oxidative stress is still on debate. In the present study, flow cytometry and cell viability assay both indicated that inhibition of SOCE with 2-APB, a well-established SOCE inhibitor [21], played a cell survival-promoting role in oxidative stress injury, which was consistent with a previous study on oxidative glutamate oxytosis [11]. STIM1, as an essential component of intact SOCE machinery [22,23], is not only be a finely tuned ER Ca^{2+} sensor, but a ROS, temperature and PH value sensors [8]. We further investigated and explicated the role of SOCE in oxidative stress by STIM1 RNAi. Similarly, inhibition of SOCE by STIM1 RNAi significantly limited H_2O_2 induced oxidative stress injury. We might conclude that STIM1-mediated SOCE played a primary role in oxidative stress injury induced by H_2O_2 insult.

Growing evidence indicated that oxidative stress induces disturbance of intracellular Ca^{2+} homeostasis, and even cell damage and death [24,25]. In neurons, intracellular Ca^{2+} overload derived from intracellular stores release and/or the extracellular space Ca^{2+} entry. Apart from voltage- and ligand-activated pathways mediate Ca^{2+} entry, SOCE is also involved in intracellular Ca^{2+} homeostasis [7]. After confirmed the protection role of SOCE inhibition on oxidative stress injury, we studied the underling relationship between Ca^{2+} overload and SOCE. Our results showed that H_2O_2 insult induced significant intracellular Ca^{2+} overload and BAPTA-AM, a kind of intracellular free-calcium chelator, significantly decreased H_2O_2-induced cytotoxicity and cell death, indicating that H_2O_2 induced oxidative stress injury is partially intracellular Ca^{2+} overload dependent. Inhibition of SOCE by using 2-APB and STIM1 RNAi significantly decreased Ca^{2+} overload peak value and delayed the peak time. Hence, we could conclude that SOCE mediated Ca^{2+} entry contributed to intracellular Ca^{2+} overload induced by H_2O_2 in HT22 cells.

As we known, mitochondria not just play a primary role in ATP production, but also function to help maintain intracellular calcium homeostasis, scavenge free radicals and regulate cell death [26–28]. Both cellular reduction–oxidation and intracellular Ca^{2+} conditions have tight relationships with mitochondrial function. MMP is critical for maintaining the physiological function of the

respiratory chain to generate ATP and the permeability of the outer mitochondrial membrane (OMM). A significant loss of MMP renders cells depleted of energy with subsequent death [27,29]. Our results showed that H_2O_2 insult induced significant loss of MMP and damage of mitochondrial membrane integrity as evidenced by increased cytosolic cytochrome C release. Meantime, the increase of Bax/Bcl-2 ratio and the activation of Caspase 3 demonstrated activation of mitochondrial apoptotic pathway after H_2O_2 insult , which was in agreed with our previous study in PC12 cells [13]. It is well known that SOCE and STIM1 are involved in the regulation of mitochondrial shape, bioenergetics and homeostasis [7,19]. Our present study showed both application of 2-APB and STIM1 RNAi could reverse the injurious effect of oxidative stress on mitochondrial function by decreasing the loss of MMP, release of cytochrome C, Bax/Bcl-2 ratio and caspase-3 activity after H_2O_2 insult, suggesting that the detrimental effects of SOCE in oxidative stress could be mediated by inducing mitochondrial dysfunction and activating mitochondrial associated apoptosis.

In conclusion, our in vitro studies investigated the possible role and mechanisms of SOCE inhibition in oxidative stress injury in HT-22 cells and the results showed that inhibition of SOCE protected HT-22 cells from H_2O_2-induced oxidative injury by alleviating intracellular Ca^{2+} overload and mitochondrial related apoptosis, indicating that inhibition of SOCE might be an important regulation target in the treatment of neurobiological disorders in which oxidative stress has been principally implicated.

Conflict of interest statement

The authors declare that there are no conflicts of interest.

Acknowledgments

We would like to give our thanks to Wenbo Liu, Jie Zhu, Juan Li, Xiaoyan Chen, and Yufen Shi for technical assistance. The work was supported by National Natural Science Foundation of China (Nos. 30930093, 81200949), research funds from goverment (Nos. AWS11J008, 2012BAI11B02) and Program for Changjiang Scholars and Innovative Research Team in University (No. IRT1053).

References

[1] J.K. Andersen, Oxidative stress in neurodegeneration: cause or consequence?, Nat Med. 10 (Suppl.) (2004) S18–S25.
[2] H. Ischiropoulos, J.S. Beckman, Oxidative stress and nitration in neurodegeneration: cause, effect, or association?, J Clin. Invest. 111 (2003) 163–169.
[3] H. Chen, H. Yoshioka, G.S. Kim, J.E. Jung, N. Okami, H. Sakata, C.M. Maier, P. Narasimhan, C.E. Goeders, P.H. Chan, Oxidative stress in ischemic brain damage: mechanisms of cell death and potential molecular targets for neuroprotection, Antioxid. Redox Signal. 14 (2011) 1505–1517.
[4] M. Bains, E.D. Hall, Antioxidant therapies in traumatic brain and spinal cord injury, Biochim. Biophys. Acta 2012 (1822) 675–684.
[5] M. Patel, Mitochondrial dysfunction and oxidative stress: cause and consequence of epileptic seizures, Free Radic. Biol. Med. 37 (2004) 1951–1962.
[6] M.V. Frantseva, J.L. Perez Velazquez, G. Tsoraklidis, A.J. Mendonca, Y. Adamchik, L.R. Mills, P.L. Carlen, M.W. Burnham, Oxidative stress is involved in seizure-induced neurodegeneration in the kindling model of epilepsy, Neuroscience 97 (2000) 431–435.
[7] N. Henke, P. Albrecht, A. Pfeiffer, D. Toutzaris, K. Zanger, A. Methner, Stromal interaction molecule 1 (STIM1) is involved in the regulation of mitochondrial shape and bioenergetics and plays a role in oxidative stress, J. Biol. Chem. 287 (2012) 42042–42052.
[8] J. Soboloff, B.S. Rothberg, M. Madesh, D.L. Gill, STIM proteins: dynamic calcium signal transducers, Nat. Rev. Mol. Cell Biol. 13 (2012) 549–565.
[9] R.K. Gandhirajan, S. Meng, H.C. Chandramoorthy, K. Mallilankaraman, S. Mancarella, H. Gao, R. Razmpour, X.F. Yang, S.R. Houser, J. Chen, W.J. Koch, H. Wang, J. Soboloff, D.L. Gill, M. Madesh, Blockade of NOX2 and STIM1 signaling limits lipopolysaccharide-induced vascular inflammation, J. Clin. Invest. 123 (2013) 887–902.
[10] I. Bogeski, T. Kilch, B.A. Niemeyer, ROS and SOCE: recent advances and controversies in the regulation of STIM and Orai, J. Physiol. 590 (2012) 4193–4200.
[11] N. Henke, P. Albrecht, I. Bouchachia, M. Ryazantseva, K. Knoll, J. Lewerenz, E. Kaznacheyeva, P. Maher, A. Methner, The plasma membrane channel ORAI1 mediates detrimental calcium influx caused by endogenous oxidative stress, Cell Death Dis. 4 (2013) e470.
[12] S. Selvaraj, Y. Sun, J.A. Watt, S. Wang, S. Lei, L. Birnbaumer, B.B. Singh, Neurotoxin-induced ER stress in mouse dopaminergic neurons involves downregulation of TRPC1 and inhibition of AKT/mTOR signaling, J. Clin. Invest. 122 (2012) 1354–1367.
[13] P. Luo, T. Chen, Y. Zhao, H. Xu, K. Huo, M. Zhao, Y. Yang, Z. Fei, Protective effect of Homer 1a against hydrogen peroxide-induced oxidative stress in PC12 cells, Free Radic. Res. 46 (2012) 766–776.
[14] Z.Y. Zhao, P. Luan, S.X. Huang, S.H. Xiao, J. Zhao, B. Zhang, B.B. Gu, R.B. Pi, J. Liu, Edaravone protects HT22 neurons from H2O2-induced apoptosis by inhibiting the MAPK signaling pathway, CNS Neurosci. Ther. 19 (2013) 163–169.
[15] T. Satoh, N. Sakai, Y. Enokido, Y. Uchiyama, H. Hatanaka, Free radical-independent protection by nerve growth factor and Bcl-2 of PC12 cells from hydrogen peroxide-triggered apoptosis, J. Biochem. 120 (1996) 540–546.
[16] A. Ishimura, K. Ishige, T. Taira, S. Shimba, S. Ono, H. Ariga, M. Tezuka, Y. Ito, Comparative study of hydrogen peroxide- and 4-hydroxy-2-nonenal-induced cell death in HT22 cells, Neurochem. Int. 52 (2008) 776–785.
[17] E. Martinez, A. Navarro, C. Ordonez, E. Del Valle, J. Tolivia, Oxidative stress induces apolipoprotein D overexpression in hippocampus during aging and Alzheimer's disease, J. Alzheimers Dis. 36 (2013) 129–144.
[18] Q. Xu, T. Konta, K. Nakayama, A. Furusu, V. Moreno-Manzano, J. Lucio-Cazana, Y. Ishikawa, L.G. Fine, J. Yao, M. Kitamura, Cellular defense against H2O2-induced apoptosis via MAP kinase-MKP-1 pathway, Free Radic. Biol. Med. 36 (2004) 985–993.
[19] B.J. Hawkins, K.M. Irrinki, K. Mallilankaraman, Y.C. Lien, Y. Wang, C.D. Bhanumathy, R. Subbiah, M.F. Ritchie, J. Soboloff, Y. Baba, T. Kurosaki, S.K. Joseph, D.L. Gill, M. Madesh, S-glutathionylation activates STIM1 and alters mitochondrial homeostasis, J. Cell Biol. 190 (2010) 391–405.
[20] R. Hooper, E. Samakai, J. Kedra, J. Soboloff, Multifaceted roles of STIM proteins, Pflugers Arch. 465 (2013) 1383–1396.
[21] M.D. Bootman, T.J. Collins, L. Mackenzie, H.L. Roderick, M.J. Berridge, C.M. Peppiatt, 2-Aminoethoxydiphenyl borate (2-APB) is a reliable blocker of store-operated Ca2+ entry but an inconsistent inhibitor of InsP3-induced Ca2+ release, FASEB J. 16 (2002) 1145–1150.
[22] J. Roos, P.J. DiGregorio, A.V. Yeromin, K. Ohlsen, M. Lioudyno, S. Zhang, O. Safrina, J.A. Kozak, S.L. Wagner, M.D. Cahalan, G. Velicelebi, K.A. Stauderman, STIM1, an essential and conserved component of store-operated Ca2+ channel function, J. Cell Biol. 169 (2005) 435–445.
[23] J. Liou, M.L. Kim, W.D. Heo, J.T. Jones, J.W. Myers, J.E. Ferrell Jr., T. Meyer, STIM is a Ca2+ sensor essential for Ca2+-store-depletion-triggered Ca2+ influx, Curr. Biol. 15 (2005) 1235–1241.
[24] M. Teepker, N. Anthes, S. Fischer, J.C. Krieg, H. Vedder, Effects of oxidative challenge and calcium on ATP-levels in neuronal cells, Neurotoxicology 28 (2007) 19–26.
[25] S.V. Avery, Molecular targets of oxidative stress, Biochem. J. 434 (2011) 201–210.
[26] J.L. Werth, S.A. Thayer, Mitochondria buffer physiological calcium loads in cultured rat dorsal root ganglion neurons, J. Neurosci. 14 (1994) 348–356.
[27] B. Zhivotovsky, S. Orrenius, Calcium and cell death mechanisms: a perspective from the cell death community, Cell Calcium 50 (2011) 211–221.
[28] M.T. Lin, M.F. Beal, Mitochondrial dysfunction and oxidative stress in neurodegenerative diseases, Nature 443 (2006) 787–795.
[29] M. Giacomello, I. Drago, P. Pizzo, T. Pozzan, Mitochondrial Ca2+ as a key regulator of cell life and death, Cell Death Differ. 14 (2007) 1267–1274.